A Most Efficient Digital Filter
The 2-Path Recursive All-pass Filter

fred harris
San Diego State University
fred.harris@sdsu.edu

*M*any of us are introduced to digital recursive filters as mappings from analog prototype structures mapped to the sample data domain by the bilinear Z-Transform. These digitals filters are normally implemented as a cascade of canonic second order filters that independently form its two poles and two zeros with two feedback and two feed forward coefficients respectively. We discuss here an alternative recursive filter structure based on simple recursive all-pass filters that use a single coefficient to form both a pole and a zero or to form two poles and two zeros. An all-pass filter has unity gain at all frequencies and otherwise exhibits a frequency dependent phase shift. We might then wonder that if the filter has unity gain at all frequencies, how it can form a stop band. We accomplish this by adjusting the phase in each path of a 2-path filter to obtain destructive cancellation of signals occupying specific spectral bands. Thus the stop-band zeros are formed by the destructive cancellation of components in the multiple paths rather than as explicit polynomial zeros. This approach leads to a wide class of very efficient digital filters that require only 25% to 50% of the computational workload of the standard cascade of canonic second order filters. These filters also permit the interchange of the resampling and filtering to obtain further workload reductions.

Introduction:
All-pass networks are the building blocks of every digital filter. All-pass networks exhibit unity gain at all frequencies and a phase shift that varies as a function of frequency. All-pass networks have poles and zeros that occur in (conjugate) reciprocal pairs. Since all-pass networks have reciprocal pole-zero pairs, the numerator and denominator are seen to be reciprocal polynomials. If the denominator is an N-th order polynomial $P_N(Z)$, the reciprocal polynomial in the numerator is $Z^N P_N(Z^{-1})$. It is easily seen that the vector of coefficients that represent the denominator polynomial is reversed to form the vector representing the numerator polynomial. A cascade of all-pass filters is also seen to be an all-pass filter. A sum of all-pass networks is not all-pass and we use these two properties to build our class our filters. Every all-pass network can be decomposed into a product of first and second order all-pass networks, thus it is sufficient to limit our discussion to first and second order filters which we refer to as type-I and type-II respectively. In this paper we limited our discussion to first and second order polynomials in Z and Z^2. The transfer functions of type-I and type-II all-pass networks are shown in equation 1 with the corresponding pole-zero diagrams shown in figure 1.

$$\begin{aligned} H_1(Z) &= \frac{(1+\alpha Z)}{(Z+\alpha)}, & H_1(Z^2) &= \frac{(1+\alpha Z^2)}{(Z^2+\alpha)}: \quad \text{TypeI} \\ H_2(Z) &= \frac{(1+\alpha_1 Z+\alpha_2 Z^2)}{(Z^2+\alpha_1 Z+\alpha_2)}, & H_2(Z^2) &= \frac{(1+\alpha_1 Z^2+\alpha_2 Z^4)}{(Z^4+\alpha_1 Z^2+\alpha_2)}: \text{TypeII} \end{aligned} \tag{1}$$

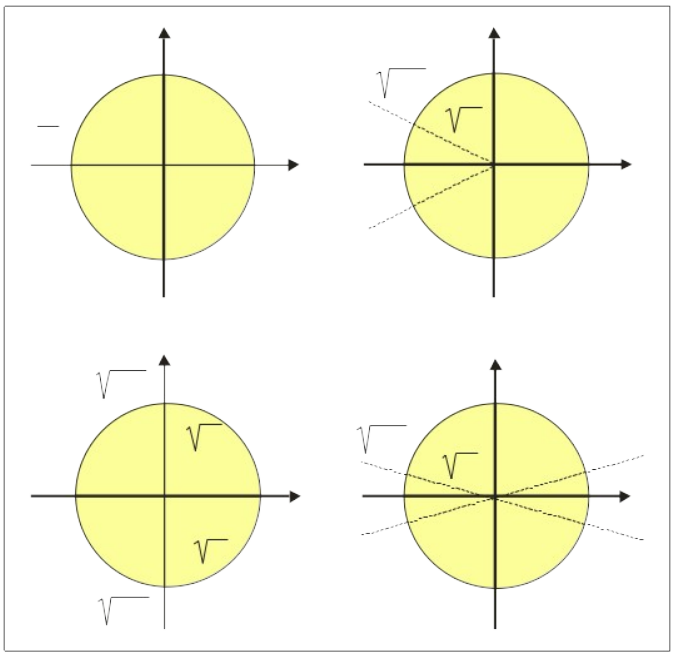

Figure 1. Pole-Zero Structure of Type-I and Type-II All-Pass Filters
of Degrees 1 and 2

Note that the single sample delay with Z-transform Z^{-1} (or 1/Z) is a special case of the type-I all pass structure obtained by setting the coefficient α to zero. Linear phase delay is all that remains as the pole of this structure approaches the origin while its zero simultaneously approaches infinity. We use the fundamental all-pass filter (Z^{-1}) as the starting point of our design process and then develop the more general case of the type-I and type-II all-pass networks to form our class of filters.

A closed form expression for the phase function of the type-1 transfer function is obtained by evaluating the transfer function on the unit circle. The result of this exercise is shown in (2).

$$\phi = -\ 2\ \mathrm{atan}\left[\frac{(1+\alpha)}{(1-\alpha)}\tan(M\,\frac{\theta}{2})\right],\quad M = 1, 2, \tag{2}$$

The phase response of the first and second order all-pass type-I structures is shown in figure 2a and 2b.

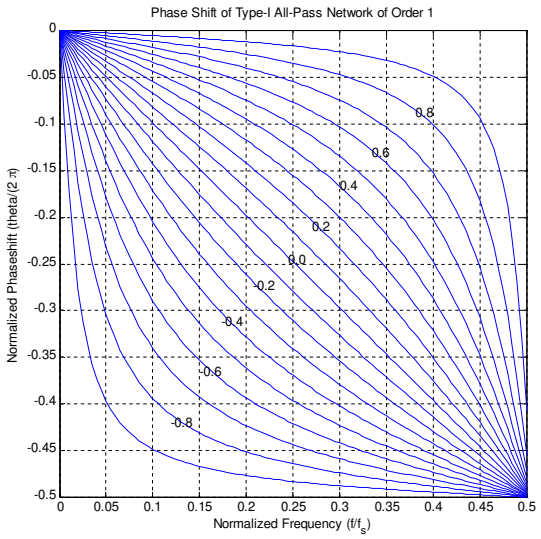

Figure 2a. Phase Response of Type-I All-Pass Filter, First Order Polynomial in Z^{-1}, as Function of Coefficient α, (α = 0.9, 0.8,….,0 ,….., -0.8, -0.9)

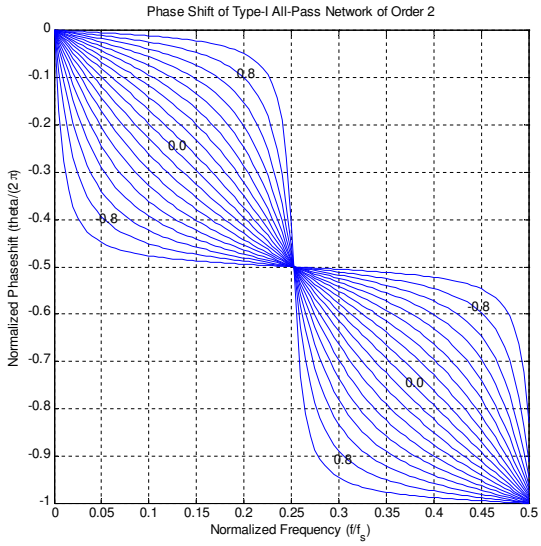

Figure 2b. Phase Response of Type-II All-Pass Filter, First Order Polynomial in Z^{-2}, as Function of Coefficient α, (α = 0.9, 0.8,….,0 ,….., -0.8, -0.9)

Note that for the first order polynomial in Z^{-1}, the transfer function for $\alpha = 0$ defaults to the pure delay, and as expected, its phase function is linear with frequency. The phase function will vary with α and this network can be thought of, and will be used as, the generalized delay element. We observe that the phase function is anchored at its end points (0 degrees at zero frequency and 180 degrees at the half sample rate) and that it warps with variation in α. It bows upward (less phase) for positive α and bows downward (more phase) for negative α. The bowing phase function permits us to use the generalized delay to obtain a specified phase shift angle at any frequency. For instance, we note that when $\alpha = 0$, the frequency for which we realize 90 degrees phase shift is 0.25 (the quarter sample rate). We can determine a value of α for which the 90 degree phase shift is obtained at any normalized frequency such as at normalized frequency 0.45 (α = 0.8) or at normalized frequency 0.05 (α = -0.73).

Implementing and Combining All-Pass Networks:
While the type-I all-pass network can be implemented in a number of architectures we limit the discussion to the one shown in figure 3. This structure has a number of desirable implementation attributes that are useful when multiple stages are placed in cascade. We observe that the single multiplier resides in the feedback loop of the lower delay register to form the denominator of the transfer function. The single multiplier also resides in the feed forward path of the upper delay register to form the numerator of the transfer function. The single multiplier thus forms all the poles and zeros of this all-pass network and we call attention to this in the equivalent processing block to the right of the filter block diagram.

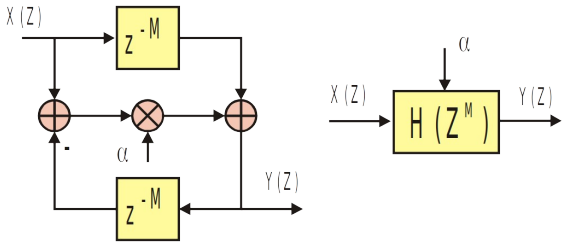

Figure 3. Single Coefficient Type-1 All-Pass Filter Structure

Two-Path Filters
While the M-th order all-pass filter finds general use in an M-path polyphase structure, we restrict our discussion in this paper to two-path filters. We first develop an understanding of the simplest two path structure and then expand the class by invoking a simple set of frequency transformations. The structure of the two path filter is presented in figure 4. Each path is formed as a cascade of all-pass filters in powers of Z^2. The delay in the lower path can be placed on either side of the all-pass network. When the filter is implemented as a multirate device the delay is positioned on the side of the filter operating at the higher of the two rates where it is absorbed by the input (or output) commutator.

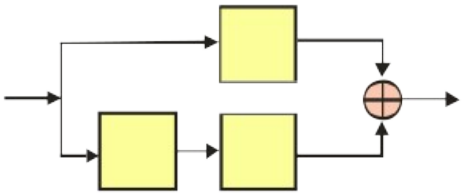

Figure 4. Two Path Polyphase Filter

This deceivingly simple filter structure offers a surprisingly rich class of filter responses. The 2-path all-pass structure can implement half-band low-pass and high-pass filters, as well as Hilbert transform filters that exhibit minimum or non-minimum phase response. The two-path filter implements standard recursive filters such as the Butterworth and the Elliptic filter. A MATLAB routine, *tony_des2* that computes the coefficients of the two-path filter and a number of its frequency transformed variants is available from the author via an e-mail request. Also, as suggested earlier, the half-band filters can be configured to embed a 1-to-2 up-sampling or a 2-to-1 down-sampling operation within the filtering process.

The prototype half-band filters have their 3-dB band edge at the quarter sample rate. All-pass frequency transformations applied to the 2-path prototype form arbitrary bandwidth low-pass and high-pass complementary filters, and arbitrary center frequency pass-band and stop-band complementary

filters. Zero packing the time response of the 2-path filter, another trivial all-pass transformation, causes spectral scaling and replication. The zero-packed structure is used in cascade with other filters in iterative filter designs to achieve composite spectral responses exhibiting narrow transition bandwidths with low-order filters.

The specific form of the prototype half-band 2-path filter is shown in figure 5. The number of poles (or order of the polynomials) in the two paths differ by precisely one, a condition assured when the number of filter segments in the lower leg is equal to or is one less than the number of filter segments in the upper leg. The structure forms complementary low pass and high pass filters as the scaled sum and difference of the two paths.

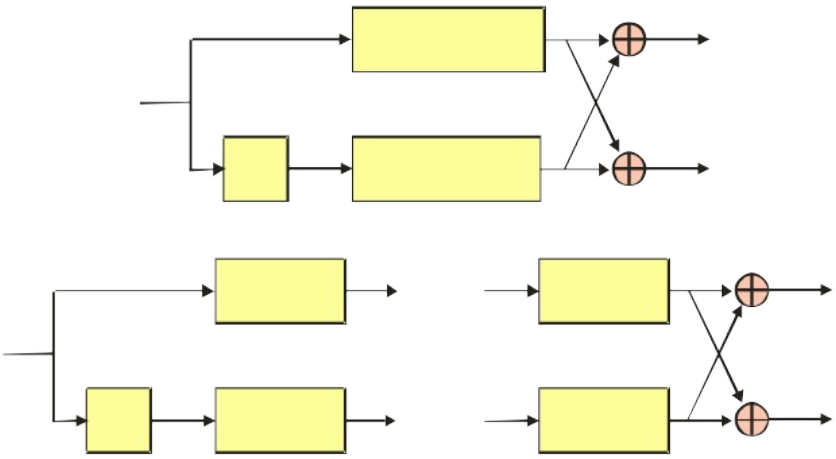

Figure 5. Two-Path All-Pass Filter

The transfer function of the 2-path filter shown in figure 5 is shown in equation (3).

$$\begin{aligned} H(Z) &= P_0(Z^2) \pm Z^{-1} P_1(Z^2) \\ P_i(Z^2) &= \prod_{k=0}^{K_i} H_{i,k}(Z^2), \quad i = 0,1 \\ H_{i,k}(Z^2) &= \frac{1+\alpha(i,k)Z^2}{Z^2+\alpha(i,k)} \end{aligned} \tag{3}$$

In particular, we can examine the simple case of two all-pass filters in each path. The transfer function for this case is shown in equation (4).

$$\begin{aligned} H(Z) &= \frac{1+\alpha_0 Z^2}{Z^2+\alpha_0}\frac{1+\alpha_2 Z^2}{Z^2+\alpha_2} \pm \frac{1}{Z}\frac{1+\alpha_1 Z^2}{Z^2+\alpha_1}\frac{1+\alpha_3 Z^2}{Z^2+\alpha_3} \\ &= \frac{b_0 Z^9 \pm b_1 Z^8 + b_2 Z^7 \pm b_3 Z^6 + b_4 Z^5 \pm b_4 Z^4 + b_3 Z^3 \pm b_2 Z^2 + b_1 Z^1 \pm b_0}{Z(Z^2+\alpha_0)(Z^2+\alpha_2)(Z^2+\alpha_3)(Z^2+\alpha_3)} \end{aligned} \tag{4}$$

We note a number of interesting properties of this transfer function, applicable to all the 2-path prototype filters. The denominator roots are on the imaginary axis restricted to the interval ± 1 to assure stability. The numerator is a linear-phase FIR filter with a symmetric weight vector. As such the numera-

tor roots must appear either on the unit circle, or if off and real, in reciprocal pairs, and if off and complex, in reciprocal conjugate quads. Thus for appropriate choice of the filter weights, the zeros of the transfer function can be placed on the unit circle, and can be distributed to obtain an equal ripple stop band response. In addition, due to the one pole difference between the two paths, the numerator must have a zero at $\pm$ 1. When the two paths are added, the numerator roots are located in the left half plane, and when subtracted, the numerator roots are mirror imaged to the right half plane forming low-pass and high-pass filters respectively.

The attraction of this class of filters is the unusual manner in which the transfer function zeros are formed. The zeros of the all-pass sub-filters reside outside the unit circle (at the reciprocal of the stable pole positions) but migrate to the unit circle as a result of the sum or difference of the two paths. The zeros appear on the unit circle because of destructive cancellation of spectral components delivered to the summing junction via the two distinct paths, as opposed to being formed by numerator weights in the feed forward path of standard biquadratic filters. The stop band zeros are a windfall. They start as the maximum phase all-pass zeros formed concurrently with the all-pass denominator roots by a single shared coefficient and migrate to the unit circle in response to addition of the path signals. This is the reason that the two path filter requires less than half the multiplies of the standard biquadratic filter.

Figure 6 presents the pole-zero diagram for this filter. The composite filter contains 9 poles and 9 zeros and requires two coefficients for path-0 and two coefficients for path-1. The *tony_des2* design routine was used to compute weights for the 9th-order filter with -60 dB equal ripple stop band. The pass-band edge is located at a normalized frequency of 0.25 and the stop-band edge that achieved the desired 60 dB stop-band attenuation is located at a normalized frequency of 0.284. This is an elliptic filter with constraints on the pole positions. The denominator coefficient vectors of the filter are listed here in decreasing powers of Z:

Path-0 Polynomial Coefficients:
Filter-0 [1 0 0.101467517]
Filter-2 [1 0 0.612422841]

Path-1 Polynomial Coefficients:
Filter-1 [1 0 0.342095596]
Filter-3 [1 0 0.867647439]

The roots presented here represent the low-pass filter formed from the 2-path filter. Figure 7 presents the phase slopes of the two paths of this filter as well as the filter frequency response. We note that the zeros of the spectrum correspond to the zero locations on the unit circle in the pole-zero diagram.

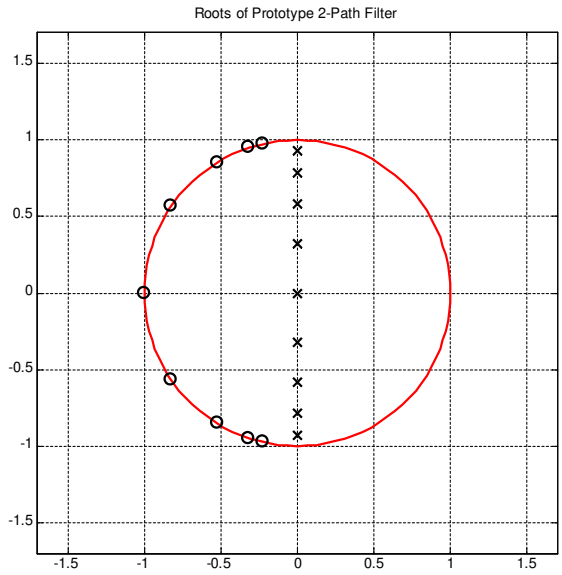

Figure 6 Pole-Zero Diagram of Two-Path, Nine-Pole, Four-Multiplier Filter

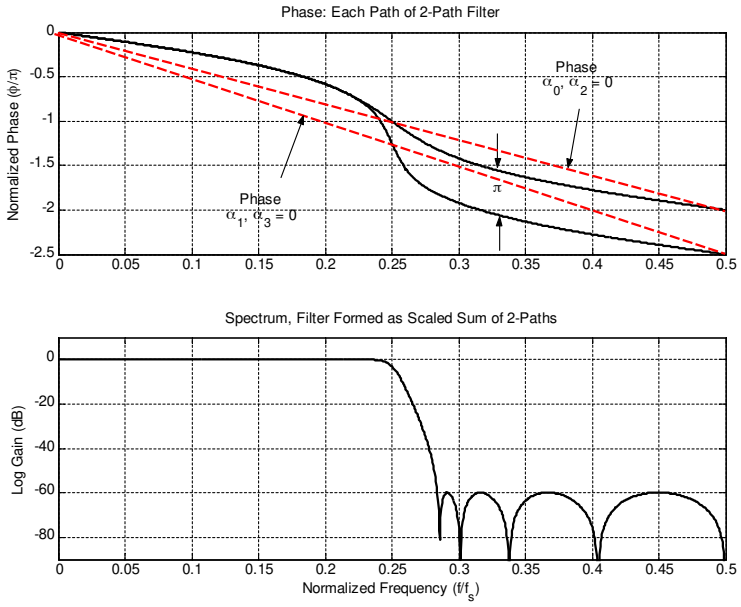

Figure 7. Two-Path Phase Slopes and Frequency response 2-Path, Nine-Pole, Four-Multiplier Filter

The first subplot in figure 7 presents two sets of phase responses for each path of the 2-path filter. The dashed lines represent the phase response of the two paths when the filter coefficients are set to zero. In this case the two paths default to 2 delays in the top path and 3 delays in the bottom path. Since the two paths differ by one delay, the phase shift difference is precisely 180 degrees at the half sample rate. When the filter coefficients in each path are adjusted to their design values, the phase response of both paths assume the bowed “lazy S” curve described earlier in figure 2b. Note that at low frequencies, the two phase curves exhibit the same phase profile and that at high frequencies, the two-phase curves maintain the same 180-degree phase difference. Thus the addition of the signals from the two paths will lead to a gain of 2 in the band of frequencies with the same phase and will result in destructive

cancellation in the band of frequencies with 180-degree phase difference. These two bands of course are the pass band and stop band respectively. We note that the two phase curves differ by exactly 180 degrees at four distinct frequencies as well as the half sample rate: these frequencies corresponding to the spectral zeros of the filter. Between these zeros, the filter exhibits stop-band side lobes that, by design, are equal ripple.

Linear Phase Two-Path Half-Band Filters

We can modify the structure of the 2-path filter to form filters with approximately linear phase response by restricting one of the paths to be pure delay. We accomplish this by setting all the filter coefficients in the upper leg to zero. This sets the all-pass filters in this leg to their default responses of pure delay with poles at the origin. As we pursue the solution to the phase matching problem in the equal-ripple approximation we find that the all-pass poles must move off the imaginary axis. In order to keep real coefficients for the all-pass filters, we call on the type-II all-pass filter structure. The lower path then contains first and second order filters in Z^2. We lose a design degree of freedom when we set the phase slope in one path to be a constant. Consequently when we design an equal-ripple group delay approximation to a specified performance we require additional all-pass sections. To meet the same out-of-band attenuation and the same stop band band-edge as the non-linear phase design of the previous section, our design routine *lineardesign*, determined that we require two first order filters in Z^2 and three second order filters in Z^2. This means that 8-coefficients are required to meet the specifications that in the non-linear phase design only required 4 coefficients. Path-0 (the delay only path) requires 16 units of delay while the all-pass denominator coefficient vector list is presented below in decreasing powers of Z which along with its single delay element form a 17-the order denominator.

Path-0 Polynomial Coefficients

Delay [zeros(1,16) 1]

Path-1 Polynomial Coefficients

Filter-0 [1 0 0.832280776]
Filter-1 [1 0 -0.421241137]
Filter-2 [1 0 0.67623706 0 0.23192313]
Filter-3 [1 0 0.00359228 0 0.19159423]
Filter-4 [1 0 -0.59689082 0 0.18016931]

Figure 8 presents the pole-zero diagram of the linear phase all-pass filter structure that meets the same spectral characteristics as those outlined in the previous section. We first note that the filter is non-minimum phase due to the zeros outside the unit circle. We also note the near cancellation of the right half plane pole cluster with the reciprocal zeros of the non-minimum phase zeros. Figure 9 presents the phase slopes of the two filter paths and the filter frequency response. We first note that the phase of the two paths is linear; consequently the group delay is constant over the filter pass band. The constant group delay matches the time delay to the peak of the impulse response which corresponds to the 16-sample time delay of the top path. Of course the spectral zeros of the frequency response coincide with the transfer function zeros on the unit circle.

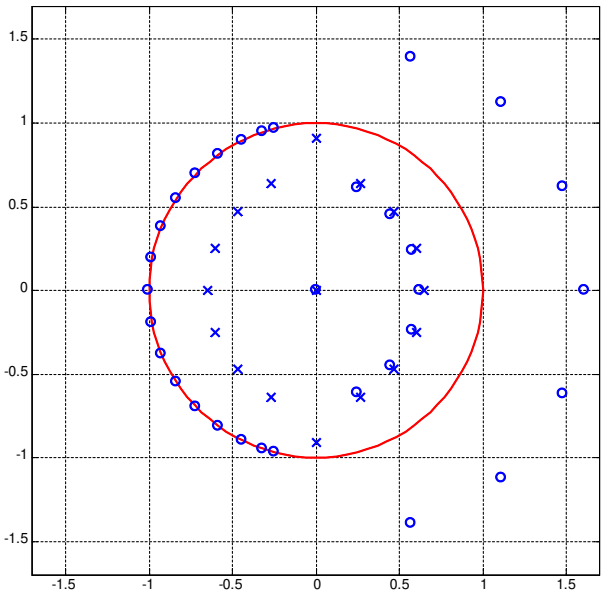

Figure 8. Pole-Zero Diagram of Two-Path, Thirty Three Pole, Eight-Multiplier Filter

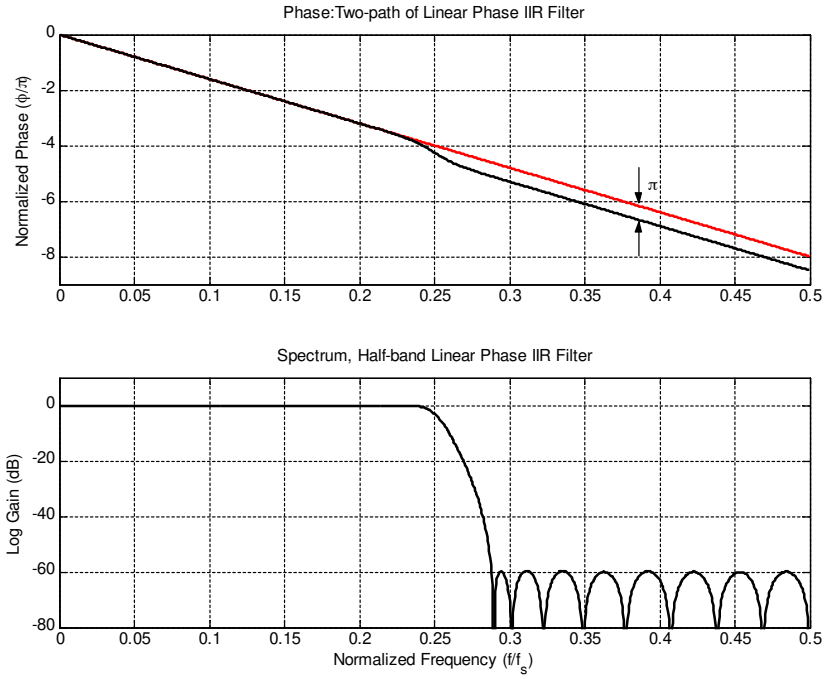

Figure 9. Two-Path Phase Slopes and Frequency Response of 2-Path, 33-Pole, 8-Multiplier Filter

Pass Band Response in Two-Path Half Band Filters

The all-pass networks that formed the half-band filter exhibit unity gain at all frequencies. These are lossless filters affecting only the phase response of signal they process. This leads to an interesting relationship between the pass-band and stop-band ripple response of the half-band filter and in fact for any of the two-path filters discussed in this paper. We noted earlier that the two-path filter presents complimentary low pass and the high pass versions of the half-band filter, the frequency responses of

which are shown in figure 10 where pass band and stop band ripples have been denoted by δ_1 and δ_2 respectively.

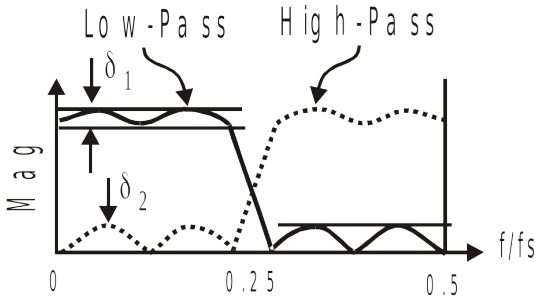

Figure 10. Magnitude Response of Low-Pass and High-Pass Half-Band Filter

The transfer functions of the low pass and of the high pass filters are shown in (5), where $P_0(Z)$ and $P_1(Z)$ are the transfer functions of the all-pass filters in each of the two paths. The power gain of the low-pass and high-pass filters is shown in (6). When we form the sum of the power gains, the cross terms in the pair of products cancel and we obtain the results shown in (7).

$$\begin{aligned} H_{LOW}(Z) &= 0.5 \cdot [P_0(Z) + Z^{-1} P_1(Z)] \\ H_{HIGH}(Z) &= 0.5 \cdot [P_0(Z) - Z^{-1} P_1(Z)] \end{aligned} \tag{5}$$

$$\begin{aligned} |H_{LOW}(Z)|^2 &= H_{LOW}(Z) H_{LOW}(Z^{-1}) \\ &= 0.25 \cdot [P_0(Z) + Z^{-1} P_1(Z)] \cdot [P_0(Z^{-1}) + Z\, P_1(Z^{-1})] \\ |H_{HIGH}(Z)|^2 &= H_{HIGH}(Z) H_{HIGH}(Z^{-1}) \\ &= 0.25 \cdot [P_0(Z) - Z^{-1} P_1(Z)] \cdot [P_0(Z^{-1}) - Z\, P_1(Z^{-1})] \end{aligned} \tag{6}$$

$$\begin{aligned} |H_{LOW}(Z)|^2 + |H_{HIGH}(Z)|^2 &= 0.25 \cdot [2 \cdot |P_0(Z)|^2 + 2 \cdot |P_1(Z)|^2] \\ &= 1 \end{aligned} \tag{7}$$

Equation (7) tells us that at any frequency, the squared magnitude of the low pass gain and the squared magnitude of the high pass gain sum to unity. This is a consequence of the filters being lossless. Energy that enters the filter is never dissipated, a fraction of it is available at the low pass output and the rest of it is available at the high pass output. This property is the reason the complementary low-pass and high-pass filters cross at their 3-dB points. If we substitute the gains at peak ripple of the low pass and high pass filters into (7), we obtain (8) which we can rearrange and solve for the relationship between $\delta_1$and δ_2. The result is interesting. We learn here that the peak to peak in-band ripple is approximately half the square of the out-of-band peak ripple. Thus if the out of band ripple is –60 dB or 1-part in a 1000, then the in-band peak to peak ripple is half of 1 part in a 1,000,000, which is on the order of 5 μ-dB (4.34 μ-dB). The half-band recursive all-pass filter exhibits an extremely small in band ripple. The in-band ripple response of the two-path 9-pole filter is seen in figure 11.

$$[1-\delta_1]^2+[\delta_2]^2=1$$
$$[1-\delta_1]=\sqrt{1-\delta_2^2}\cong 1-0.5\cdot\delta_2^2 \qquad (8)$$
$$\delta_1\cong 0.5\cdot\delta_2^2$$

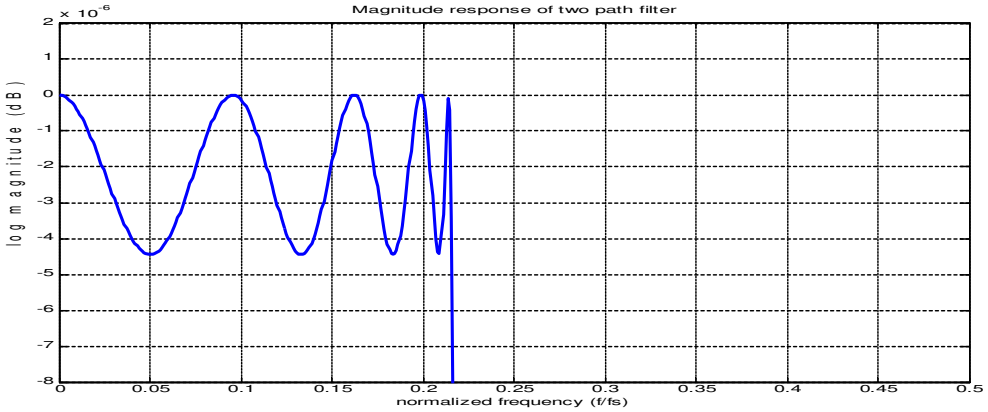

Figure 11. In-Band Ripple Level of Two-path, Nine-Pole Recursive Filter

Transforming the Prototype Half Band To Arbitrary Bandwidth

In the previous section we examined the design of two-path half-band filters formed from recursive all-pass first-order filters in the variable Z^2. We did this because we have easy access to the weights of this simple constrained filter, the constraint being stated in equation (5). If we include a requirement that the stop band be equal ripple, the half band filters we examine are elliptic filters that can be designed from standard design routines. Our program *Tony_des2* essentially does this in addition to the frequency transformations we are about to examine. The prototype half-band filter can be transformed to form other filters with specified (arbitrary) bandwidth and center frequency. In this section, elementary frequency transformations are introduced and their impact on the prototype architecture as well as on the system response is reviewed. In particular the frequency transformation that permits bandwidth tuning of the prototype is introduced first. Additional transformations that permit tuning of the center frequency of the prototype filter are also discussed.

Low-Pass To Low-Pass Transformation

We now address the transformation that converts a low-pass half-band filter to a low-pass arbitrary-bandwidth filter. Frequency transformations occur when an existing all-pass sub network in a filter is replaced by another all-pass sub network. In particular, we present the transformation shown in (9).

$$\frac{1}{Z}\Rightarrow\frac{1+bZ}{Z+b};\quad b=\frac{1-\tan(\theta_b/2)}{1+\tan(\theta_b/2)};\quad \theta_b=2\pi\frac{f_b}{f_S} \qquad (9)$$

This is the generalized delay element we introduced in the initial discussion of first-order all-pass networks. We can physically replace each delay in the prototype filter with the all-pass network and then tune the prototype by adjusting the parameter “b”. We have fielded many designs in which we perform this substitution. Some of these designs are cited in the bibliography. For the purpose of this paper we perform the substitution algebraically in the all-pass filters comprising the two-path half-band filter, and in doing so generate a second structure for which we will develop and present an appropriate architecture.

We substitute (9) into the first order, in Z^2, all-pass filter introduced in (2) and rewritten in (10),

$$G(Z) = H(Z^2)\Big|_{Z \Rightarrow \frac{Z+b}{1+bZ}}$$
$$G(Z) = \frac{1+\alpha Z^2}{Z^2+\alpha}\Bigg|_{Z \Rightarrow \frac{Z+b}{1+bZ}} \tag{10}$$

After performing the indicated substitution and gathering terms, we find the form of the transformed transfer function is as shown in (11).

$$G(Z) = \frac{1+c_1 Z + c_2 Z^2}{Z^2 + c_1 Z + c_2}; \quad c_1 = \frac{2b(1+\alpha)}{1+\alpha b^2} \quad c_2 = \frac{b^2+\alpha}{1+\alpha b^2} \tag{11}$$

As expected, when $b \Rightarrow 0, c_1 \Rightarrow 0, \text{and } c_2 \Rightarrow \alpha,$ the transformed all-pass filter reverts back to the original first-order filter in Z^2. The architecture of the transformed filter, which permits one multiplier to form the matching numerator and denominator coefficient simultaneously, is shown in figure 12. Also shown is a processing block G(Z) that uses two coefficients c_1 and c_2. This is seen to be an extension of the one-multiply structure presented in figure 3. The primary difference in the two architectures is the presence of the coefficient and multiplier c_1 associated with the power of Z^{-1}. This term, formerly zero, is the sum of the polynomial roots, and hence is minus twice the real part of the roots. With this coefficient being non-zero, the roots of the polynomial are no longer restricted to the imaginary axis.

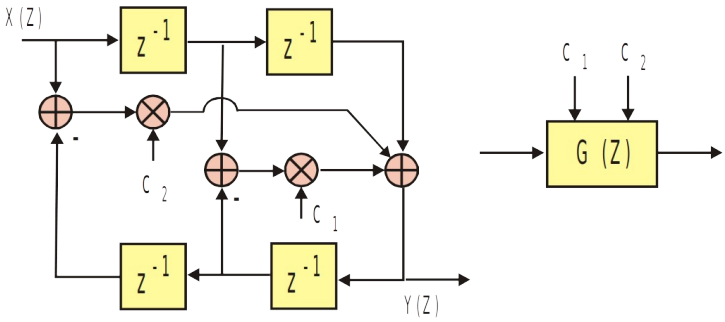

Figure 12. Block Diagram of General Second Order All-Pass Filter

The root locations of the transformed, or generalized second-order all-pass filter, are arbitrary except that they appear as conjugates inside the unit circle, and the poles and zeros appear in reciprocal sets as indicated in figure 13.

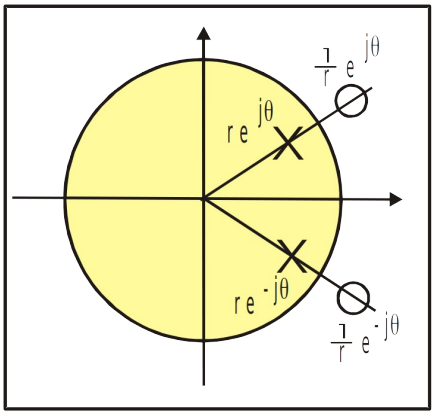

Figure 13 Pole Zero Diagram of Generalized Second Order All-Pass Filter

The two-path prototype filter contained one or more one-multiply first order recursive filters in Z^2 and a single delay. We effect a frequency transformation on the prototype filter by applying the low-pass to-low pass transformation shown in (10). Doing so converts the one-multiply first-order in Z^2 all-pass filter to the generalized two-multiply second-order all-pass filter and converts the delay, a zero-multiply all-pass filter to the generalized one-multiply first-order in Z all-pass filter. Figure 14 shows how applying the frequency transformation affects the structure of the prototype. Note that the 9-pole, 9-zero half-band filter, which is implemented with only 4 multipliers, now requires 9 multipliers to form the same 9-poles and 9-zeros for the arbitrary-bandwidth version of the two-path network. This is still significantly less than the standard cascade of first and second-order canonic filters for which the same 9-pole, 9-zero filter would require 23 multipliers.

Figure 15 presents the pole-zero diagram of the frequency transformed prototype filter. The 9-poles have been pulled off the imaginary axis, and the 9-zeros have migrated around the unit circle to form the reduced-bandwidth version of the prototype. Figure 16 presents the phase response of the two paths and the frequency response obtained by applying the low-pass to low-pass frequency transformation to the prototype two-path, four-multiply, half-band filter presented in figure 7. The low-pass to low-pass transformation moved pass band-edge from normalized frequency 0.25 to normalized frequency 0.1.

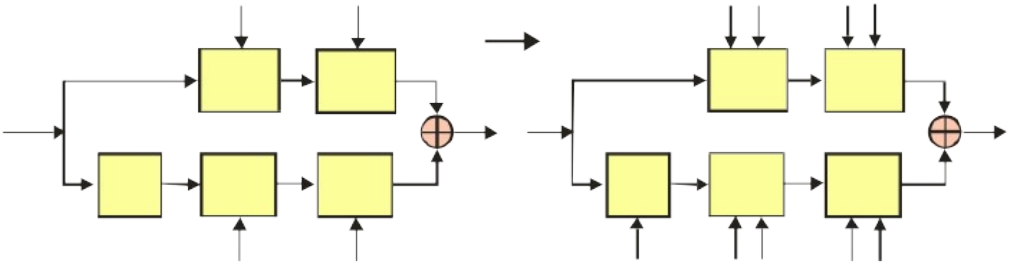

Figure 14. Effect on Architecture of Frequency Transformation Applied to Two-Path Half-Band All-Pass Filter

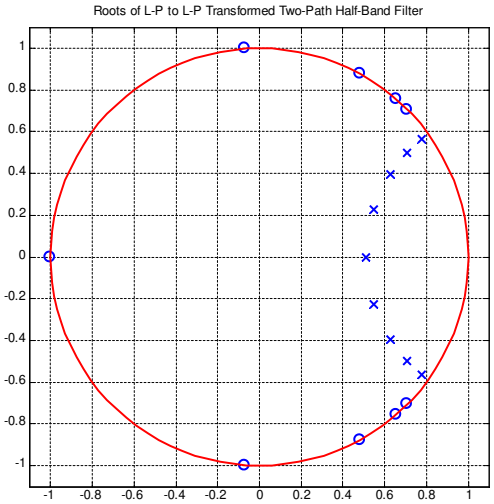

Figure 15. Pole-Zero Diagram Obtained by Frequency Transforming Half-Band Filter to Normalized Frequency 0.1.

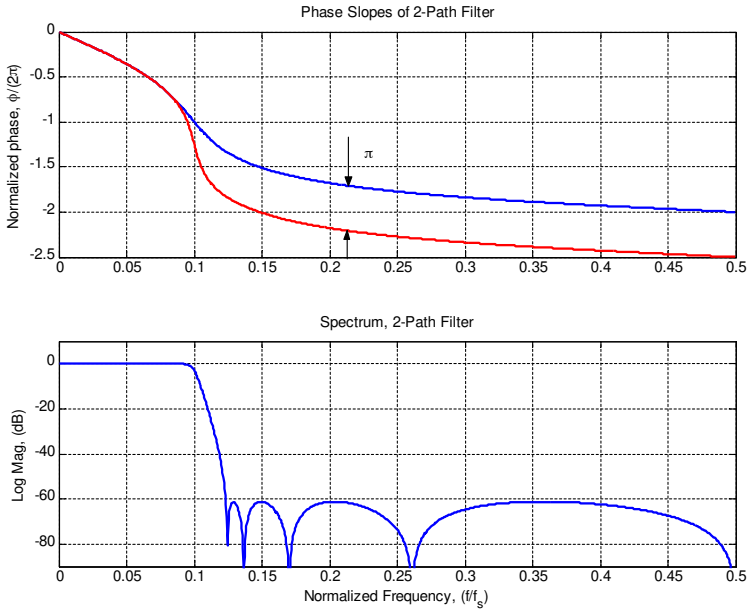

Figure 16. Phase Response of Two Paths and Frequency Response of 2-Path Half-Band Filter Frequency Transformed to 0.1 Normalized Bandwidth

Low-Pass to Band-Pass Transformation

In the previous section we examined the design of two-path, arbitrary-bandwidth low-pass filters formed from recursive all-pass first and second order filters as shown in figure 14. We formed this filter by a transformation of a prototype half-band filter. We now address the second transformation, one that performs the low-pass to band-pass transformation. As in the previous section we invoke a frequency transformation wherein an existing all-pass sub network in a filter is replaced by another all-pass sub network. In particular, we now examine the transformation shown in (12).

$$\frac{1}{Z} \Rightarrow -\frac{1}{Z}\frac{1-cZ}{Z-c};\quad c=\cos(\theta_C);\quad \theta_C = 2\pi\frac{f_C}{f_S} \tag{12}$$

This, except for the sign, is a cascade of a delay element with the generalized delay element we introduced in the initial discussion of first-order all-pass networks. We can physically replace each delay in the prototype filter with this all-pass network and then tune the center frequency of the low-pass prototype by adjusting the parameter c. For the purpose of this paper we perform the substitution algebraically in the all-pass filters comprising the two-path pre-distorted arbitrary-bandwidth filter, and in doing so generate yet a third structure for which we will develop and present an appropriate architecture. We substitute (12) into the second-order all-pass filter derived in (11) and rewritten in (13).

$$\begin{aligned} F(Z) &= G(Z)\Big|_{Z\Rightarrow\frac{Z(Z-c)}{(cZ-1)}} \\ &= \frac{(b^2+\alpha)+2b(1+\alpha)Z+(1+\alpha b^2)Z^2}{(1+\alpha b^2)+2b(1+\alpha)Z+(b^2+\alpha)Z^2}\Bigg|_{Z\Rightarrow\frac{Z(Z-c)}{(cZ-1)}} \end{aligned} \tag{13}$$

After performing the indicated substitution and gathering up terms, we find the form of the transformed transfer function is as shown in (14).

$$\begin{aligned} F(Z) &= \frac{1+d_1Z+d_2Z^2+d_3Z^3+d_4Z^4}{Z^4+d_1Z^3+d_2Z^2+d_3Z+d_4} \\ d_1 &= \frac{-2c(1+b)(1+\alpha b)}{1+\alpha b^2} \quad d_2 = \frac{(1+\alpha)(c^2(1+b)^2+2b)}{1+\alpha b^2} \\ d_3 &= \frac{-2c(1+b)(1+\alpha b)}{1+\alpha b^2} \quad d_4 = \frac{\alpha+b^2}{1+\alpha b^2} \end{aligned} \tag{14}$$

As expected, when we let $c \Rightarrow 0$, d_1 and $d_3 \Rightarrow 0$, while $d_2 \Rightarrow c_1$ and $d_4 \Rightarrow c_2$, the weights default to those of the prototype (arbitrary-bandwidth) filter. The transformation from low pass to band pass generates two spectral copies of the original spectrum, one each at the positive and negative tuned center frequency. The architecture of the transformed filter, which permits one multiplier to simultaneously form the matching numerator and denominator coefficients, is shown in Figure 17. Also shown is a processing block F(Z) which uses four coefficients d_1, d_2, d_3 and d_4. This is seen to be an extension of the two-multiply structure presented in figure 14.

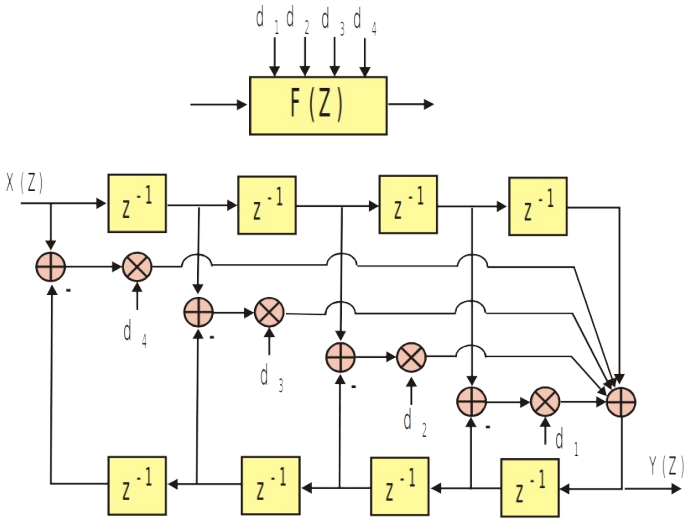

Figure 17. Block Diagram of General Fourth Order All-Pass Filter

We have just described the low-pass to band-pass transformation that is applied to the second-order all-pass networks of the two-path filter. One additional transformation that requires attention is the low-pass to band-pass transformation that must be applied to the generalized delay or bandwidth-transformed delay from the prototype half-band filter. We substitute (12) into the first-order all-pass filter derived in (9) and rewritten in (15).

$$E(Z) = \left.\frac{1+bZ}{Z+b}\right|_{Z \Rightarrow \frac{Z(Z-c)}{(cZ-1)}} = \frac{(cZ-1)+bZ(Z-c)}{Z(Z-c)+b(cZ-1)} = \frac{-1+c(1-b)Z+bZ^2}{Z^2-c(1-b)Z-b} \tag{15}$$

As expected, when $c \Rightarrow 1$, the denominator goes to (Z+b)(Z-1) while the numerator goes to (1+bZ)(Z-1) so that the transformed all-pass filter reverts back to the original first-order filter. The distributed minus sign in the numerator modifies the architecture of the transformed second-order filter by shuffling signs in figure 13 to form the filter shown in figure 18. Also shown is a processing block E(Z) which uses two coefficients e_1 and e_2.

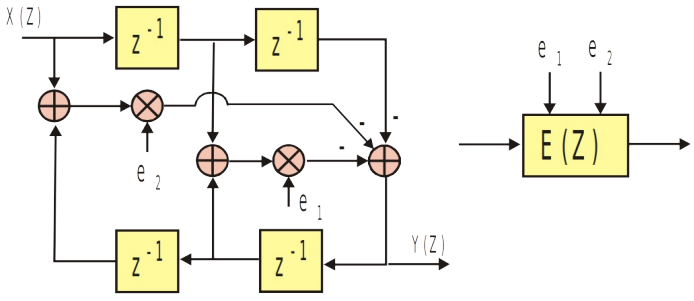

Figure 18. Block Diagram of Low-Pass to Band-Pass Transformation Applied to Low-Pass to Low-Pass Transformed Delay Element

In the process of transforming the low-pass filter to a band-pass filter we convert the two-multiply second-order all-pass filter to a four-multiply fourth-order all-pass filter, and convert the one-multiply low-pass-to-low-pass filter to a two-multiply all-pass filter. The doubling of the number of multiplies is the consequence of replicating the spectral response at two spectral centers of the real band-pass system. Note that the 9-pole, 9-zero arbitrary low-pass filter now requires 18 multipliers to form the 18-poles and 18-zeros for band-pass version of the two-path network. This is still significantly less than the standard cascade of first and second-order canonic filters for which the same 18-pole, 18-zero filter would require 45 multipliers. Figure 19 shows how the structure of the prototype is affected by applying the low-pass to band-pass frequency transformation.

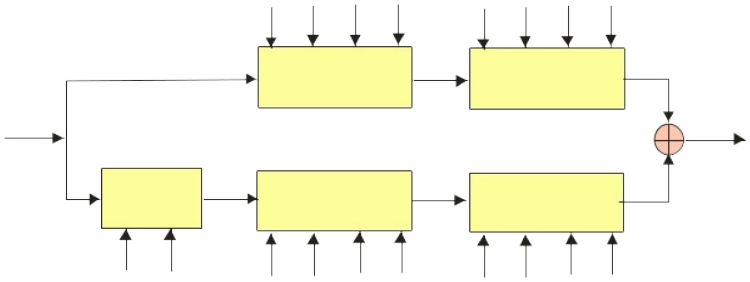

Figure 19. Effect on Architecture of Low-Pass to band-Pass Frequency Transformation Applied to Two-Path Arbitrary bandwidth All-Pass Filter

Figure 20 presents the pole-zero diagram of the frequency-transformed prototype filter. The 9-poles defining the low-pass filter have been pulled to the neighborhood of the band-pass center frequency. The 9-zeros have also replicated, appearing both below and above the pass-band frequency. Figure 21 presents the phase response of the two paths and the frequency response obtained by applying the low-pass to band-pass frequency transformation to the prototype two-path, 9-multiply, low-pass filter presented in figure 14. The one-sided bandwidth was originally adjusted to a normalized frequency of 0.1, and is now translated to a center frequency of 0.22.

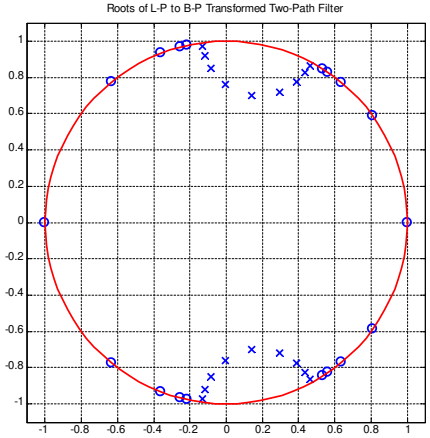

Figure 20. Pole-Zero Plot of Two-Path All-Pass Half-Band Filter Subjected to Low-Pass to Low-Pass and then Low-Pass to Band-Pass Transformations

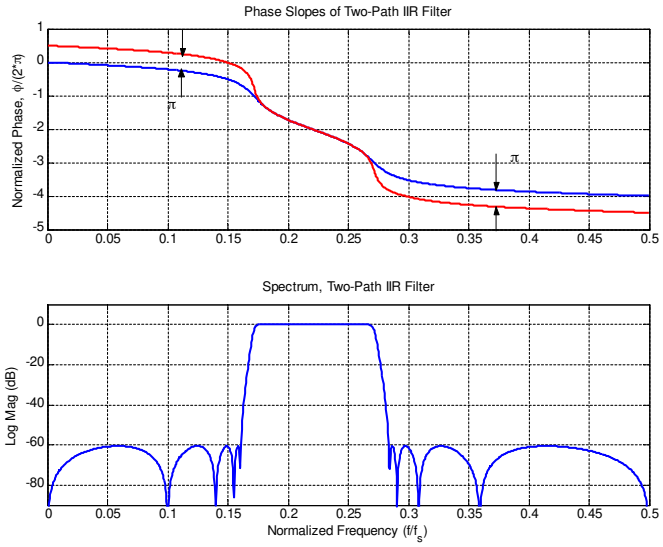

Figure 21. Frequency Response of Two-Path All-Pass Filter Subjected to Low-Pass to Low-Pass and then Low-Pass to Band-Pass Transformations

Summary

We have presented a class of particularly efficient recursive filters based on two-path recursive all-pass filters. The numerator and denominator of an all-pass filter have reciprocal polynomials with the coefficient sequence of the denominator reversed in the numerator. The all-pass filters described in this paper fold and align the numerator registers with the denominator registers so that the common coefficients can be shared and thus form a pole and reciprocal zero with a single multiply. Coefficients are selected via a design algorithm to obtain matching phase profiles in specific spectral intervals with 180 degree phase offsets in other spectral intervals. When the time series from the two paths are added, the signals residing in the spectral intervals with 180 degree phase offsets are destructively cancelled. From the transfer function perspective, the non minimum phase zeros in the separate numerators migrate to the unit circle as a result of the interaction of the numerator-denominator cross products resulting when forming the common denominator from the separate transfer functions of the two paths. The migration to the unit circle of the essentially free reciprocal zeros, formed while building the system poles, is the reason this class of filters requires less than half the multiplies of a standard recursive filter. The destructive cancellation of the spectral regions defined for the two-path half-band filter is preserved when the filter is subjected to transformations that enable arbitrary band width and arbitrary center frequencies. The one characteristic not preserved under the transformation is the ability to embed 1-to-2 or 2-to-1 multirate processing in the two path filter. The extension of the 2-path filter structure to an M-path structure with similar computational efficiency is the topic of a second presentation.

Bibliography:

Ansari, R. and B. Liu “Efficient Sampling Rate Alteration Using Recursive (IIR) Digital Filters”, IEEE Trans. On Acoustics, Speech, and Signal Processing, Vol. 31, Dec. 1983, pp. 1366-1373.

Drews, W. and L. Gaszi, “A New Design Method for Polyphase Filters Using All-Pass Sections”, IEEE Trans. On Circuits and Systems, Vol. 33, Mar. 1986, pp 346-348.

Dick, Chris, and harris, fred, On the Structure, Performance, and Applications of Recursive All-Pass Filters with Adjustable and Linear Group Delay, ICASSP '02, 2002 IEEE International Conference on Acoustics, Speech, and Signal Processing,Vol.2, pp. 1517-1520

harris, fred, Multirate Signal Processing for Communication Systems, Englewood Cliff, NJ, Prentice-Hall Inc., 2004.

harris, fred. “On the Design and Performance of Efficient and Novel Filter Structures Using Polyphase Recursive All-Pass Filters”, Keynote Presentation ISSPA-92 (International Symposium on Signal Processing) Gold Coast, Australia 16–21 August 1992

harris, fred, and Eric Brooking, “A Versatile Parametric Filter Using an Imbedded All-Pass Sub-Filter to Independently Adjust Bandwidth, Center Frequency, and Boost or Cut”, 95th Audio Engineering Society (AES) Convention, New York, New York, 7-10 October 1993

harris, fred, Bob Caulfied, and Bill McKnight, “Use of All-pass Networks to Tune the Center Frequency of Sigma Delta Modulators”, 27th Asilomar Conference on Signals, Systems, and Computers, Pacific Grove, CA., 31 October to 3 November 1993

harris, fred, Itzhak Gurantz, and Shimon Tzukerman “Digital (T/2) Low pass Nyquist Filter Using Recursive All-pass Polyphase Resampling Filter for Signaling Rates 10 kHz to 10 MHz”, 26th Annual Asilomar Conference on Signals, Systems, and Computers, Pacific Grove, CA., 26–28 October 1992

harris, fred, Maximilien d’Oreye de Lantramange and A.G. Constantinides, “Design and Implementation of Efficient Resampling Filters Using Polyphase Recursive All-Pass Filters”, 25th Annual Asilomar Conference on Signals, Systems, and Computer, Pacific Grove, CA., 4–6 November 1991

Jovanovic-Dolecek, Gordana. Multirate Systems: Design and Applications, London, Idea Group, 2002.

Krukowski, A.; Kale, I.;Constraint Two-Path Polyphase IIR Filter Design Using Downhill Simplex Algorithm, The 2001 IEEE International Symposium on Circuits and Systems, 2001, ISCAS 2001, 6-9 May 2001 Vol. 2, pp.749-752

Krukowski, A.; Kale, I.; Polyphase IIR Filter Banks for Subband Adaptive Echo Cancellation Application, Proceedings of the 2003 International Symposium on Circuits and Systems, ISCAS '03.,25-28 May 2003, Vol. 4, pp. IV-405-408.

Krukowski, A.; Kale, I.; The Design of Arbitrary-Band Multi-Path Polyphase IIR Filters, The 2001 IEEE International Symposium on Circuits and Systems, ISCAS 2001, 6-9 May 2001, vol. 2, pp.741-744.

Mitra, Sanjit, Neuvo, Yrjo, and Roivainen Hannu, Design of Recursive Digital Filters with variable Characteristics, International Journal of Circuit Theory and Applications, 1990, Vol. 18, 107-119

Mok, F.; Constantinides, A.G.; Cheung, P.Y.K., A Flexible Decimation Filter Architecture for Sigma-Delta Converters, IEE Colloquium on Oversampling Techniques and Sigma-Delta Modulation, 30 Mar 1994,pp. 5/1-6

Regalia, Phillip, Mitra, Sanjit, and Vaidyanathan, P. P., The Digital All-Pass Filter: A Versatile Signal processing Building Block, Proceedings of the IEEE, Vol. 76, No. 1, Jan 1988, pp19-36

Renfors, M. and T. Saramaki, “Recursive N-th Band Digital Filters, Parts I and II”, IEEE Trans. CAS, Vol. 34, pp. 24-51, January 1987.

Vaidyanathan, P. P. Multirate Systems and Filter Banks, Englewood Cliff, NJ, Prentice-Hall Inc., 1993.

Valenzuela R. A. and Anton Constantinides, "Digital Signal Processing Schemes for Efficient Interpolation and Decimation", IEE Proceedings, Dec 1983, Vol. 130, Pt. G, No. 6, pp. 225-235